OPEN ACCESS Freely available online

PLoS one

An Unusual Helix Turn Helix Motif in the Catalytic Core of HIV-1 Integrase Binds Viral DNA and LEDGF

Hayate Merad[1], Horea Porumb[1], Loussiné Zargarian[1], Brigitte René[1], Zeina Hobaika[1], Richard G. Maroun[2], Olivier Mauffret[1], Serge Fermandjian[1]*

1 LBPA, CNRS (UMR 8113)–Ecole Normale Supérieure de Cachan, Cachan, France, **2** Département des Sciences de la Vie et de la Terre, Faculté des Sciences, Université Saint Joseph, CST-Mar Roukos, B. P. 1514, Beyrouth, Liban

Abstract

Background: Integrase (IN) of the type 1 human immunodeficiency virus (HIV-1) catalyzes the integration of viral DNA into host cellular DNA. We identified a bi-helix motif (residues 149–186) in the crystal structure of the catalytic core (CC) of the IN-Phe185Lys variant that consists of the α_4 and α_5 helices connected by a 3 to 5-residue turn. The motif is embedded in a large array of interactions that stabilize the monomer and the dimer.

Principal Findings: We describe the conformational and binding properties of the corresponding synthetic peptide. This displays features of the protein motif structure thanks to the mutual intramolecular interactions of the α_4 and α_5 helices that maintain the fold. The main properties are the binding to: 1- the processing-attachment site at the LTR (long terminal repeat) ends of virus DNA with a K_d (dissociation constant) in the sub-micromolar range; 2- the whole IN enzyme; and 3- the IN binding domain (IBD) but not the IBD-Asp366Asn variant of LEDGF (lens epidermal derived growth factor) lacking the essential Asp366 residue. In our motif, in contrast to the conventional HTH (helix-turn-helix), it is the N terminal helix (α_4) which has the role of DNA recognition helix, while the C terminal helix (α_5) would rather contribute to the motif stabilization by interactions with the α_4 helix.

Conclusion: The motif, termed HTHi (i, for inverted) emerges as a central piece of the IN structure and function. It could therefore represent an attractive target in the search for inhibitors working at the DNA-IN, IN-IN and IN-LEDGF interfaces.

Citation: Merad H, Porumb H, Zargarian L, René B, Hobaika Z, et al. (2009) An Unusual Helix Turn Helix Motif in the Catalytic Core of HIV-1 Integrase Binds Viral DNA and LEDGF. PLoS ONE 4(1): e4081. doi:10.1371/journal.pone.0004081

Editor: Ashley M. Buckle, Monash University, Australia

Received October 17, 2008; **Accepted** December 4, 2008; **Published** January 1, 2009

Funding: This work was supported by the Centre National de la Recherche Scientifique (CNRS), the French-Libanese program CEDRE (05 SF21/L14) and in part by grants from SIDACTION and the National Agency for Research against AIDS (ANRS) (to H. M.). The funders had no role in study design, data collection and analysis, decision to publish, or preparation of the manuscript.

Competing Interests: The authors have declared that no competing interests exist.

* E-mail: serge.fermandjian@lbpa.ens-cachan.fr

Introduction

The integration of the HIV-1 genome into the host cell chromosome is mediated by the viral integrase (IN) [1–6]. The enzyme catalyzes a multi-step reaction i.e., 3′-end processing and strand transfer, to integrate a linear DNA copy (cDNA) of the retroviral genome into the host cell DNA [2,7,8]. The retroviral DNA integration mimics that of insertion elements and bacteriophage Mu transposons [9–11] and bears resemblance to the RAG1/2 recombinase [12].

The HIV-1 IN is essential for the viral life cycle and is therefore an attractive target for developing anti-HIV drugs [13,14]. The enzyme (288 amino acid residues, 32 kDa) has three well defined structural domains: an N terminal domain (residues 1 to 49), a central catalytic domain or catalytic core, CC (residues 50 to 212), and a C terminal domain (residues 213 to 288) [15–17]. Several crystal structures of the CC domain and of two-domain fragments (CC domain linked either to the C terminal domain or the N terminal domain) have been already resolved by X-ray crystallography [18–25] while the N terminal and C terminal domains have been analyzed in solution by NMR [26,27]. Each domain, taken separately, forms a dimer and this is true also true for the N terminal-CC and the C terminal CC bi-domains [18–29]. The CC dimer (Fig. 1a) is organized around a two fold axis with a large interface involving, in particular, helices α_1 and α_5 (residues 172–184) [18,30]. Other retroviral IN CC structures display the same dimer boundary, indicating that this type of interface is biologically relevant.

Actually, cross-linked dimers have been shown to be active for 3′-processing and single end integration [31]. Yet, a large number of data suggest that the tetramer is the form stabilizing the synaptic complexes of IN with the two viral DNA ends and appears to be the form required for the strand transfer [32–37]. Several theoretical models of the DNA-IN complexes have proven the relevance of tetramers to position the viral and cellular DNA partners at reactive distance [38–41].

The CC domain is organized in five β-strands surrounded by six α helices (α_1 to α_6), and contains a highly conserved catalytic D, $DX_{35}E$ motif embedded in a protein RNase H fold [17,20,21]. The amphipathic α_4 helix, (residues 148–167), which protrudes at the protein surface, bears the catalytic residue Glu-152 and several other residues, such as Gln-148, Lys-156 and Lys-159, which have been shown to be important for the binding of IN to DNA and for virus survival. In the crystal structure of CC bound to the inhibitor

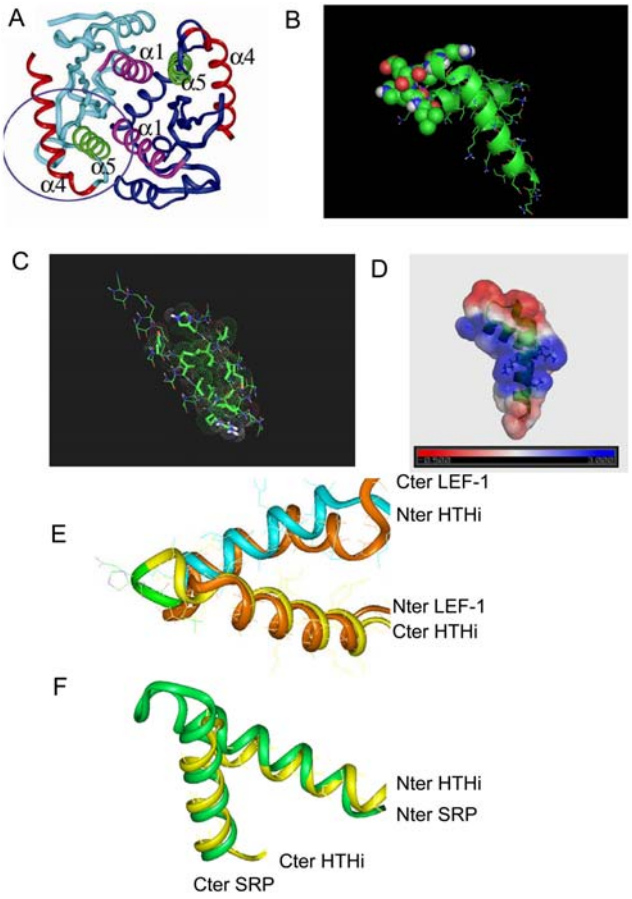

Figure 1. Identification of an "inverted" HTH motif (HTHi) at the catalytic core surface of integrase (PDB ID 1BIU [20]). a). Crystal structure of the catalytic core domain, associated into a dimer. **b**). Representation of the HTHi motif, with the loop residues shown by van der Waals spheres. **c).** The side chain residues involved in intramolecular contacts, shown by sticks and van der Waals spheres. **d).** The electrostatic potential at the solvent-accessible surface; the Lys-156, Lys-159 and Lys-160 residues are shown by sticks. **e**). HTHi motif of IN, superimposed onto the "classical" HTH motif of the HMG (highly mobile group) protein LEF-1 (lymphoid enhancer binding factor, PDB ID 2LEF, brown). **f**). HTHi motif of IN, superimposed onto the HTHi motif of the Signal Recognition Particle (PDB ID 2FFH, green).
doi:10.1371/journal.pone.0004081.g001

5CITEP (1-(5-chloroindol-3-yl)-3-(tetrazoyl)-1, 3-propanedione enol) among the six protein-drug interactions, five involve amino acid side chains of the α_4 helix [42], confirming the relevance of the α_4 helix to IN function [41,43–47].

The propensity of IN to associate and form aggregates is the main barrier to the study of its structure and interactions by physical-chemical means including the widely used x-rays and NMR techniques. To date the only detailed depiction of the IN-DNA complex is provided by molecular modeling [38–41]. To overcome the difficulties inherent to the use of the entire enzyme we decided to dissect its properties and to analyze it part by part. Our laboratory has previously shown, in line with a systematic search by Li et al. [48], that peptides deriving from the α_4 helix had inhibitory activity against IN [49,50]. This was also the case for peptides reproducing the sequences of the α_1 and α_5 helices involved in the CC dimer interface (α_1:$\alpha_{5'}$ and $\alpha_{1'}$:α_5) [30]. We have also shown that the peptide region 163–171, encompassing both the turn and the N and C terminal parts of the α_4 and α_5 helices, respectively, was a strong epitope and antibodies refined against this region inhibited both the 3′ processing and strand transfer reactions in *in vitro* assays [49]. Interestingly, the epitope region, in particular the residue Gln168 important for turn integrity, IN dimer formation and virus replication, has been shown to share hydrogen bonds with the IBD (IN binding domain) of LEDGF/p75 (lens epidermal derived growth factor), a transcriptional coactivator that is also an essential HIV integration cofactor *in vivo* [49,51–56]. Moreover, it has been assumed that the peptide region 161–173 superposing our epitope was involved in the nuclear import of IN [57], since a peptide reproducing this sequence caused the active nuclear import of BSA tethered to it [57,58]; the matter was somehow reassessed in so far as the fact that Val-165 and Arg-166 did not play the anticipated specific roles in the nuclear localization of HIV-1 pre-integration complex [59,60].

Actually, the α_4 and α_5 helices form a stable bi-helix fold at the protein surface of the CC crystal structure (Fig.1a–f). This recalls the well-known HTH (helix-turn-helix) motif of proteins specialized in DNA recognition [61]. Such motifs are generally associated with biological functions, protein structures and even evolutionary history. To assess the possible role of this bi-helix in IN we carried out an analysis of the structural and binding properties of the corresponding synthetic peptide (residues Gly-149 to Lys-186) using circular dichroism (CD) [43] and fluorescence. The peptide dealt with in this work represents the sequence found in the IN-CC Phe185Lys variant (Table 1a). It has been logically preferred to the native wt sequence (Table 1a) because it is the Phe185Lys variant that was used in the various crystallizations [20] and co-crystallizations so far reported [42,52]. The Phe185Lys mutation is not expected to affect the interactions with LTR and LEDGF IBD [51,52]. We have nevertheless performed a number of experiments (not shown here) to verify that the structure of the wt bi-helix was similar to that of the mutant.

Generally, the HTH motifs are strongly influenced by their context within the proteins and often lose their original biological functions when they are isolated from their protein environment. Here, we show that the isolated HTH motif continues to fulfill three of the major functions of the whole parental enzyme: i) it recognizes the U5LTR extremity of viral DNA at the attachment-processing site in a specific manner i.e., it preserves its viral DNA binding property; ii) it self-associates and associates to IN i.e., it reproduces some of the enzyme oligomerisation behavior, and iii) it binds to the IBD of LEDGF but not to its Asp366Asn-IBD variant lacking the essential Asp366 residue i.e., it maintains its ability to interact with specific partners.

Results

The HTHi conformation

The bi-helix motif we focus on (α_4 helix-turn-α_5 helix) occurs in the peptide segment from Gly-149 to Lys-186 of the IN-Phe185Lys variant. Like many classical HTH motifs, this bi-helix is exposed at the protein surface where it is largely accessible to solvent, proteins, DNA and organic ligands (Fig. 1a) [20]. The two helices are linked by a flexible turn of 3 to 5 residues bringing the amphipathic α_4 helix (situated in N terminal position) onto the C terminal α_5 helix through an angle of about 120°(Fig. 1b). The helices interact with each other through 16 mainly hydrophobic side chain–side chain contacts (Fig. 1c and Table 2). The juxtaposition of the helices generates a positive electrostatic potential exposed at the solvent accessible surface (Fig. 1d). The only difference between the present motif and the standard HTH motif is the inversion of position of the DNA recognition helix (α_4 helix) and of the so-called stabilizing helix (α5) (Fig. 1e). Actually, the bi-helix motif of IN resembles the RNA-recognizing motif of

Table 1. Sequences of Peptides and Oligonucleotides.

Peptides*	wt HTHi	SQG$_{149}$VIESMNK$_{156}$ELKKIIGQVRDQ$_{168}$AEHLKTAVQMAV**W**IHNF$_{185}$K
	HTHi	**Y**G$_{149}$VIESMNK$_{156}$ELKKIIGQVRDQ$_{168}$AEHLKTAVQMAVFIHN**K**$_{185}$K**A**
	α_4	SQG$_{149}$VVESMNK$_{156}$ELKKIIGQVR**Y**
	K156	SQ**A**$_{149}$**KL**E**E**MNK$_{156}$ELKK**LLA**QVR**A**Q$_{168}$**W**
	INH5	DQ$_{168}$AEHLKTAVQMAVFIHN**Y**$_{185}$K**A**
Oligonucleotides **	LTR34	$_5$'-ACTGCTAGAGATTTTCC**TTT**GGAAAATCTCTAGCAGT-$_{3'}$
	LTR34f5′	$_5$'-$_f$ACTGCTAGAGATTTTCC**TTT**GGAAAATCTCTAGCAGT-$_{3'}$
	LTR34fm	$_5$'-ACTGCTAGAGATTTTCC**TFT**GGAAAATCTCTAGCAGT-$_{3'}$
	CRE	$_5$'-$_f$GAGATGACGTCATCTC-$_{3'}$

*The HTHi peptide reproduces the Gly-149 to Lys-186 sequence of HIV-1 IN Phe185Lys [20]. The loop region is underlined. The mutated residues are in bold characters. An N-terminal labeled carboxyfluorescein derivative of HTHi was also used (not shown). The peptides α_4, K156 and INH5 were dealt with in [30,43,50].

**The LTR34 oligonucleotides are designed to adopt a hairpin conformation, as already reported [43]. The hairpins contain a 17 bp stem, reproducing the HIV-1 U5LTR end, and a loop formed by three thymine nucleotides (TTT in bold characters). The fluorescein reporter group, f, is grafted either to the 5′ extremity (LTR34f5′, CRE) or to the central T residue (F) of the loop (LTR34fm).

doi:10.1371/journal.pone.0004081.t001

the SRP (Signal Recognition Particle, Fig. 1f), where the role of the helices are inverted, the N terminal one recognizing the DNA and the C-terminal one stabilizing the structure [62]. The bi-helix motif was therefore hereafter called HTHi (helix-turn-helix inverted).

The comparison of the GOR IV [63] and AGADIR [64] predictions strongly suggest that long distance interactions–like those stabilizing the protein tertiary structures–are needed besides the short distance interactions in order to keep the helix secondary structure in the HTHi motif (Fig. 2). Examination of the reported crystal structures shows that long range interactions occur in great number inside the HTHi motif itself i.e., between the α_4 and the α_5 helices (there are 16 such interactions, listed in Table 2), but also between the HTHi motif and other components of the protein (for example, there are 16 interactions between HTHi and the neighboring β-sheet–Table 2). Accordingly, a loss of helicity could be feared upon isolation of the motif from the protein context.

CD analysis indicates that the secondary structure of the HTHi peptide in solution is strongly concentration dependent. At 6 μM, with its two negative bands at 208 nm and 222 nm, the CD spectrum of HTHi reflects a helical content of 10–15% (full line curve in Fig. 3). Upon increasing the peptide concentration to 25 μM, the CD spectrum manifests an important change. This is illustrated by the reduction of the broad negative band at 222 nm,

Table 2. Main interactions within HTHi (helices α_4 and α_5) and of HTHi with the neighbouring β-sheet in the IN catalytic core (data from PDB ID 1BIU, [20]).

		α_4-helix											**β-sheet**			
		V150	**I151**	**M154**	**N155**	**E157**	**L158**	**I161**	**I162**	**V165**	**R166**	**Q168**	**Y83**	**I84**	**A86**	**V88**
	L172								Φ		Φ					
	A17$_5$								Φ		Φ					
	V176								Φ						Φ	Φ
	Q177														H	
	M178									Φ		Φ				
α_5-helix	A179						Φ	Φ	Φ							
	V180						Φ								Φ	
	I182							Φ		Φ						
	H183					E		Φ								
	N184												Φ	Φ		
	I186					E										
	Q62	Φ	Φ													
	N64		Φ		E/H											
β-sheet	L68								Φ							
	I73								Φ							
	V75				Φ		Φ									
	I84			Φ			Φ									

ϕ: hydrophobic contacts; H: hydrogen bonds; E: Electrostatic interactions.

doi:10.1371/journal.pone.0004081.t002

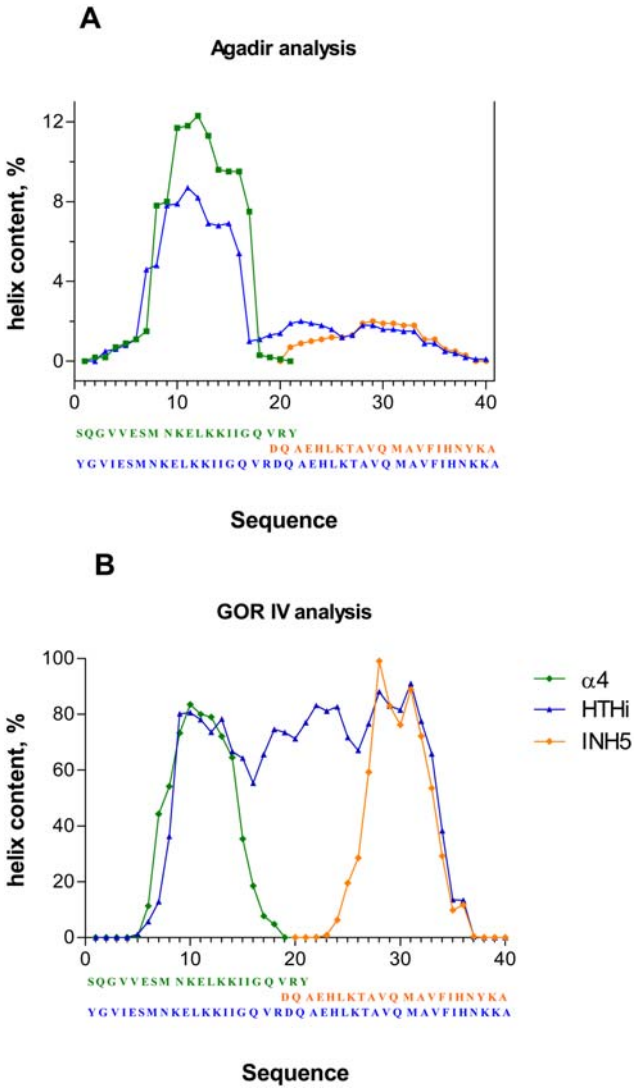

Figure 2. Secondary structure predictions. Results provided by: **a**). Agadir [64] and **b**). GOR IV [63] for the helical propensities of HTHi (blue), α_4 (green) and INH5 (orange). The predictions with Agadir were performed at pH 7, at a temperature of 25°C.
doi:10.1371/journal.pone.0004081.g002

together with the replacement of the negative band at 208 nm by a larger band mostly centered at 198 nm that bears a component with positive tendency at 190 nm, signaling the presence of a weak amount of helix (dotted line curve in Fig. 3).

The above CD experiments reveal the propensity of HTHi to form oligomers in solution at high concentration. It appears that the setting up of intermolecular interactions occurs at the detriment of the intramolecular interactions between the α_4 and the α_5 helices and impairs the stability of the HTHi fold and consequently that of the of the helix secondary structure. We argue that the weakening of these intramolecular interactions is the main cause leading to a decrease of the helix content of the motif at high peptide concentration.

The stabilization of the HTHi fold by the intramolecular interactions between the α_4 and α_5 helices is highlighted by the comparison of the CD spectrum of HTHi with the spectra of its component peptides, α_4 and INH5 (inset to Figure 3). The fact that the helix content of HTHi is greater than that of peptides α_4 [43] and INH5 [30] is particularly obvious in the low-wavelength region of the CD spectra. Indeed, while the separate components of the bi-helix show important negative bands in the 195 nm domain of the spectrum, this feature vanishes in the spectrum of HTHi, which develops a positive band below 190 nm, compatible with a helical structure.

Binding of the HTHi motif to viral DNA

We carried out CD and fluorescence experiments to demonstrate that peptide HTHi binds with a good affinity to the viral LTR DNA.

To begin with, CD was used to assess the conformational changes undergone by the HTHi peptide upon interacting with LTR34 DNA (Table 1). Indeed, the latter exerts a helix stabilizing effect that is attested in the difference spectrum (i.e., peptide-DNA complex minus DNA) by the increase of the positive band at 190 nm and of the two negative bands at 208 and 222 nm, less perceptible in the spectra of unbound HTHi (Fig. 3). The HTHi motif practically doubles its helical content when binding to LTR34. This behavior is not unique: we have already shown that a peptide derived from the b-ZIP (basic-zipper) motif of the c-jun protein manifested the same helix stabilization upon binding to DNA [65].

The binding parameters were determined by fluorescence anisotropy measurements. A representative binding isotherm illustrating the titration of the oligonucleotide LTR34fm (Table 1b), by peptide HTHi is shown in Fig. 4a. The binding curve is biphasic, whereas that obtained with the structural analog LTR34f5′ is monophasic. With LTR34fm, each plateau indicates the saturation of an interaction. The first, corresponding to the high affinity binding, has been assigned to the specific recognition by HTHi of the extremity of viral DNA [43]. The high affinity is abolished by the grafting of the fluorescein moiety at the 5′extremity (LTR34f5′) (Fig. 4a). The dissociation constants of peptide HTHi, determined by curve fitting, are $K_{d1} = 0.05$ μM and $K_{d2} = 1.9$ μM for LTR34fm and $K_d = 2.9$ μM for LTR34f5′ (Fig. 4a). Note that the non-specific binding to the negative control sequence (CRE, cAMP response element) is within this latter range of affinities ($K_d = 6.6$ μM).

Interaction of the HTHi motif with wt IN

In a previous study, based on the intrinsic fluorescence properties of IN conferred by its six Trp residues, we have shown the ability of peptide INH5 (Table 1a) to interact with IN with a concentration midpoint ($C_{0.5}$) of 168 nM [30]. The interaction, occurring at the $\alpha_{1'}$:α_5/α_1:$\alpha_{5'}$ interface, caused the dissociation of the tetramers and dimers of IN [30]. The experiments performed with HTHi under conditions similar to those we had previously used for peptide INH5 [30], show that HTHi interacts with wt IN (at 100 nM monomer concentration) with a $C_{0.5}$ value of 104 nM, while the peptide α_4, taken alone, binds to wt IN with a $C_{0.5}$ value of 53 nM (Fig. 3b). Indeed, we had previously shown that peptide α_4 interacted with IN likely by forming a coiled-coil structure with its counterpart in the protein [50,66].

Interaction of the HTHi motif with LEDGF

Fluorescence anisotropy was also used to asses the binding of the HTHi motif to IBD-LEDGF. A fluorescein-labeled HTHi peptide (Fig. 4c) was prepared for this purpose and titrated by both the wt and the Asp366Asn mutated LEDGF IBD protein ligands. It has been previously shown that Asp366 is essential for the binding of LEDGF to IN [52,54]. The overall pattern unambiguously shows that only the wt IBD binds HTHi. Curve analysis provides a K_d of the order of 12 μM. We find that HTHi reproduces the properties of the CC of IN in so far as the recognition of LEDGF is

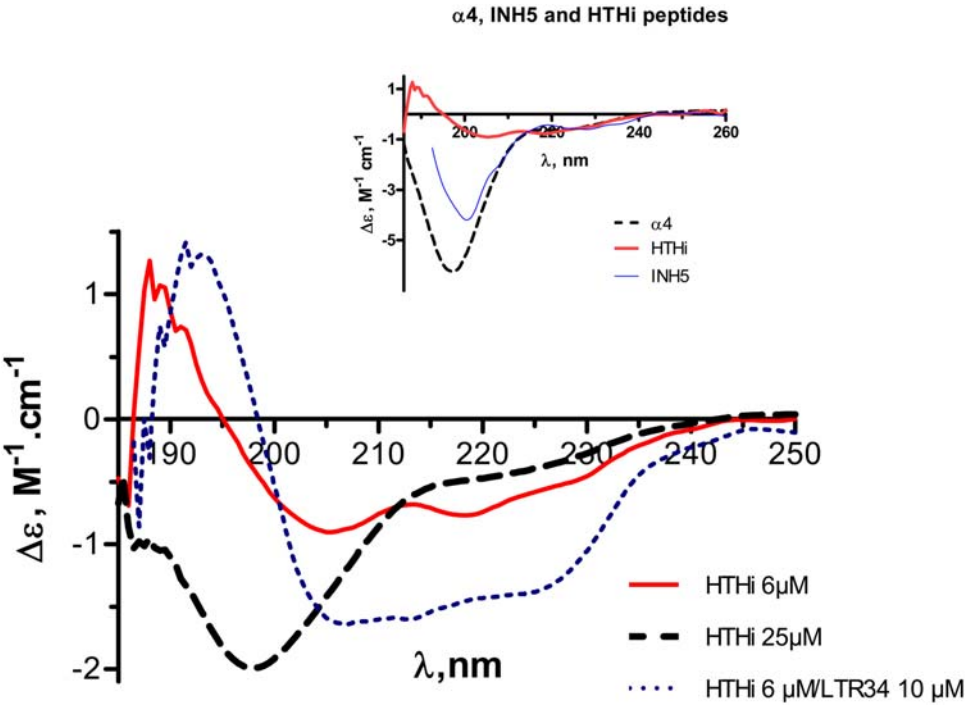

Figure 3. Circular dichroism. Spectra of peptide HTHi at 6 μM (—, red) and at 25 μM (—, black), and difference spectrum of the complex [HTHi (6 μM)+LTR34 (10 μM)] minus the CD spectrum of LTR34 (10 μM) (**……**, blue). Insert: CD spectrum of HTHi compared to the spectra of its component peptides, α_4 (after Figure 6 in [43]) and INH5 (after Figure 3b in [30]). Recall that INH5 comprises both the α_5 helix and the turn linking α_5 to α_4 (Table 1a).
doi:10.1371/journal.pone.0004081.g003

concerned. The essential role of the IBD residue Asp-366 in the interaction is confirmed.

Discussion

The so-called HTHi motif (α4-turn-α5) identified at the IN protein surface presents an unexpected multiplicity of functions revealed by the study of the corresponding synthetic HTHi peptide. In the latter, hydrophobic contacts between its α_4 and α_5 arms confer stability to the ensemble, i.e., to the tertiary structure and the helical secondary structure. The α_4 helix is more basic than the α_5 helix, which is consistent with its DNA binding property. However, only a stable preformed scaffold permits the proper spatial orientation of the interactive amino acid side chains and their adjustment onto their complementary nucleotides of the DNA target without large conformational change and therefore large consumption of energy. This improves the affinity and confers specificity to the binding.

Our results strongly suggest that helix stability in the HTHi motif is essential to the specific recognition of viral DNA. In particular, the α_4 peptide taken in isolation, which does not benefit of the HTHi stabilizing context, is a very poor DNA binder. The difference of DNA binding affinity between the peptides HTHi and α_4 can be attributed to the larger conformational change that the latter must undergo in order to adopt the bound helical conformation.

In a previous work we pointed out the importance of the conformational entropy in the binding of the α_4 helix to the viral DNA. In order to reduce this effect, we had designed an analog of the α_4 peptide that had its secondary structure stabilized by helicogenic mutations (Gly149Ala, Ile161Leu, Ile162Leu and Gly163Ala). The resulting peptide, K156, was a good mimic of the α_4 helix in the protein context and was better organized for binding than peptide α_4. The use of peptide K156 with the oligonucleotide LTR34fm permitted the identification of a high affinity site ($K_{d1} = 2.1$ nM), corresponding to the attachment site of the enzyme on the six outermost bases of viral DNA and of a low affinity site in the micromolar range ($K_{d2} = 54$ μM) corresponding to the non-specific binding of IN[43]. The grafting of the bulky fluorescein at the 5′ extremity (LTR34f5; Table 1b), i.e., at a position in close proximity to the 3′-processing site, suppressed the high affinity binding mode of K156 but preserved the low affinity mode. The absence of effect on the binding to the low affinity site from the grafted fluorescein suggested that this site was distant on the DNA from the high affinity site [43].

The behavior of peptide HTHi is similar to that of peptide K156. With HTHi there are two binding modes as well, one with a low dissociation constant in the nanomolar range ($K_{d1} = 50$ nM) and the other with a high dissociation constant in the micromolar range ($K_{d2} = 1.9$ μM), in the case of LTR34fm; and there is only one binding mode in the micromolecular range ($K_d = 2.9$ μM) in the case of LTR34f5′ (Fig. 4a). The non-specific binding of peptide HTHi to the negative control sequence, CRE, is within this latter range of affinities; $K_d = 6.6$ μM. ; comparatively, that of peptide K156 was 16 μM [43].

Thus, the two peptide ligands, HTHi and K156, present the same DNA binding properties. The two binding modes, of which the first appears specific for the intact processing-attachment site of LTR DNA, are present in the two cases, albeit with different affinities. The role of conformation is noteworthy. Peptide K156, whose secondary structure has largely benefited from helicogenic mutations, manifests a greater affinity for viral DNA than peptide HTHi, in which the α_4 helix component, certainly stabilized by its interactions with the α_5 helix, is nevertheless less stable than

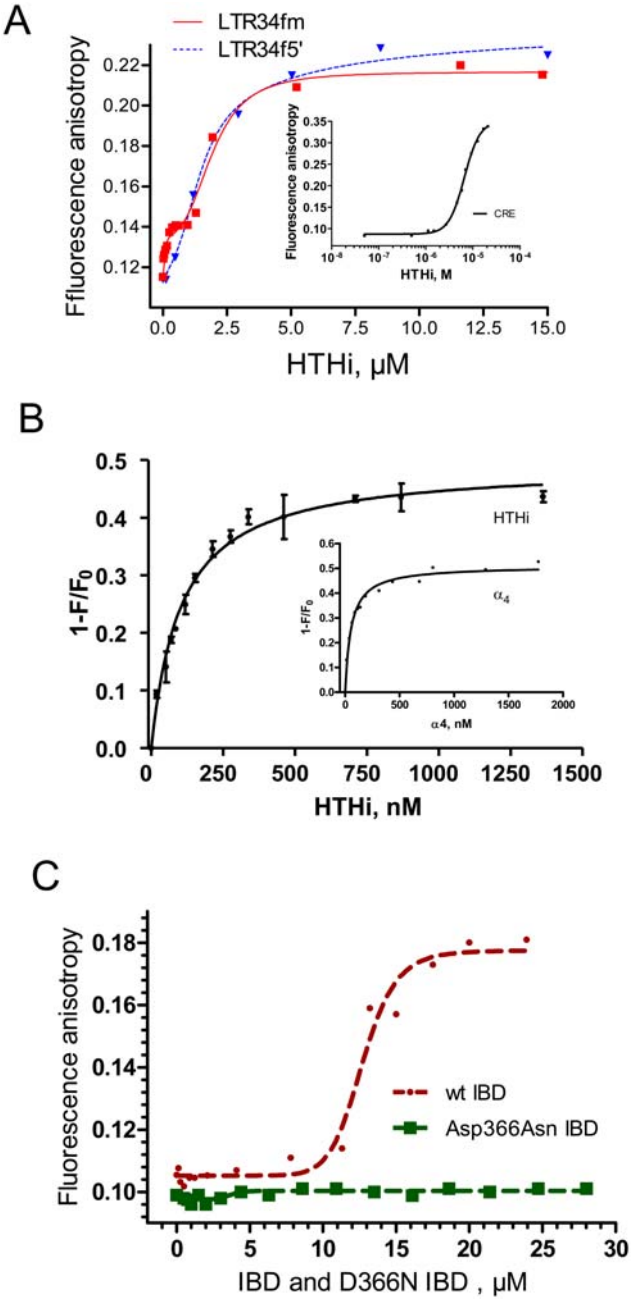

Figure 4. Fluorescence. a). Interaction with DNA. Fluorescence anisotropy titration by peptide HTHi of LTR34fm (squares, red) and LTR34f5′ (triangles, blue). Inset: titration of CRE by peptide HTHi. In all cases, the fluorescein-labeled DNA was at 20 nM. The K_d values obtained by curve fitting (with ±10% uncertainty) are: 0.05 μM and 1.9 μM for LTR34fm; 2.9 μM for LTR34f5′; and 6.6 μM for CRE. **b). Interaction with wt IN**. Quenching of the intrinsic fluorescence of wt IN by peptide HTHi. Inset: Titration of wt IN by peptide α_4. In all cases, the wt IN monomer concentration was 100 nM. The midpoints of the titration curves are at 104±8 nM and 53±5 nM for peptides HTHi and α_4 respectively. **c). Interaction with LEDGF-IBD**. Fluorescence anisotropy titration of fluorescein-grafted HTHi peptide (50 nM) by LEDGF-IBD (wt IBD, round symbols, and mutated IBD, squares). The K_d of the wt IBD-HTHi interaction is 12.3±0.3 μM, with a Hill number of 11±3.

doi:10.1371/journal.pone.0004081.g004

peptide K156. This is consistent with the idea of a higher preformed conformation for binding of peptide K156 compared with peptide HTHi that lowers the entropy cost of interaction of the former. As a corollary, the isolated peptide α_4, which mostly displays random conformation because of the absence of either helicogenic mutations in its sequence or helix stabilization conferred by the interaction with α_5, is completely unable to specifically bind the viral DNA.

X-ray crystallographic studies of the co-crystal of CC with 5CITEP also illustrate the importance of the HTHi α_4 helix in the IN enzyme. Results strongly suggest that the a4 helix would be the primary target of the DKA (diketo acid/aryl) family of inhibitors of IN acting on the 3′ processing step [14,42,67]. In the complex, the drug interacts with five residues of the α_4 helix and at least four of them (Lys-156, Lys-159, Gln-148 and Glu-152) are also implicated in the stabilization of the viral DNA-CC complex [14,43].

Concerning the role of the α_5 helix, it is clear from the various crystal structures that it participates to both the dimerization of the enzyme and the stabilization of the motif [18–29]. There are examples in the literature showing that the so-called stabilizing helix of HTH motifs is involved in the protein dimerization. This is the case of topoisomerase II, in which the binding site to DNA is fashioned from the interaction of two HTH motifs [68]. The implication of the α_5 helix in the enzyme structure and activity has been highlighted in our previous report showing that peptide INH5, which comprises the α_5 helix, inhibits IN by dissociating the IN dimers and tetramers [30].

The role of the HTHi motif is not limited to that of its α_4 and α_5 helix components. At the solvent accessible surface, in the center of the motif, the electrostatic potential is uniform and positive and it changes sign at the turn connecting the α_4 and α_5 helices (Fig. 1d). The 161–173 region is a strong epitope and also a protein binder [49,51–56]. Antibodies enriched against this epitope inhibit both the 3′ processing and the strand transfer reaction [49]. The particular variation of the electrostatic potential at the solvent accessible surface in that region is compatible with these functions. As a matter of fact, a peptide corresponding to the epitope region has been shown to mediate the nuclear import of the covalently linked serum albumin [58], although this region has been incorrectly proposed as being a possible NLS (nuclear localization signal) [57]. Nevertheless, the present results confirm the propensity of the epitope region to associate with important proteins, such as LEDGF. The co-crystal structure of CC bound to LEDGF-IBD shows that the epitope region is recognized by LEDGF. The formation of a complex between IN and LEDGF is biologically relevant and is a prerequisite to the strand transfer into the cell chromosome [51–56]. In the complex, there are numerous stabilizing contacts, such as those involving the α_3 helix and a portion of the α_1 helix, but it is the turn region of HTHi (residues Glu-170, His-171 and Gln-168) that makes the major contribution, particularly in binding the hotspot residue Asp-366 and the residue Ile-365 of LEDGF[51,52,54]. Our results are compatible with these findings. Resembling the IN CC, the peptide HTHi binds wt IBD, but not its Asp366Asn variant. We are thus allowed to conclude that the pattern of interactions found in the CC-IBD crystal is still present in the peptide HTHi-IBD complex.

All together, the results mentioned above indicate that the HTHi motif identified in IN behaves like a multifunctional entity. Being involved in enzyme oligomerisation (via its α_5 helix), in LTR end recognition (via its α_4 helix) and in binding to LEDGF (via the turn region, which also acts as a strong epitope), it emerges as a central piece of both the IN structure and activity. Moreover, the α_4 helix of HTHi could be the target of inhibitors belonging to the DKA family, as suggested by the crystal structure of 5 CITEP

bound to IN CC [14,42,67]. We propose that HTHi could constitute a reliable model for the study of new inhibitors acting at the IN-IN, the IN-DNA and the IN-LEDGF interfaces. This issue will be further addressed possibly by looking for peptidomimetics to the α_4 and α_5 helices, as well as to the epitope region–with the aim of transforming them into therapeutic agents.

Materials and Methods

Peptides

We used the synthetic peptides shown in Table 1a. They were made according to the Fmoc procedure, as already reported for peptide α_4, for its "stabilized" analogue i.e., peptide K156, and for the peptide INH5, derived from the α_5 helix [30,43]. Peptide α_4 reproduces the α_4 helix sequence of IN; peptide K156 is a variant of the α_4 peptide resulting from the replacement of weakly helicogenic residues by more helicogenic ones in several biologically irrelevant positions [43]; peptide INH5 contains both the α_5 helix and the turn connecting the α_5 helix to the α_4 helix [30]. The peptides HTHi and wt HTHi reproduce the sequences of the HTHi motifs in the IN-Phe185Lys variant and in wt IN respectively. A version of the HTHi peptide with a carboxyfluorescein at the N-terminus has also been prepared. Tyr or Trp aromatic residues, when absent in the native sequences, were purposely added in order to enable peptide quantification by UV absorption spectra. Peptide concentrations were determined using a molar absorption coefficient at 280 nm equal to 1 280 M^{-1} cm^{-1} for the tyrosine-containing peptides α_4, INH5 and HTHi and 5600 M^{-1} cm^{-1} for the tryptophane-containing peptides K156 and wt IN.

DNA oligonucleotides

The oligonucleotides (Table 1b) were purchased from Cybergene ESGS (France) and Eurogentec (Belgium). The choice of monomolecular hairpin-forming oligonucleotides, rather than bimolecular duplex-forming ones, was motivated by the need for stability under the low concentrations inherent to the fluorescence anisotropy experiments. The fluorescein reporter group is grafted either to the central T nucleotide (LTR34fm) or to the 5′ extremity (LTR34f5′ and CRE). The CRE (cAMP responsive element) sequence was used as negative control. The version of LTR34 without fluorescein was used in CD studies.

Proteins

Fluorescence titrations were performed with the wild-type IN (wt IN) [69]. The presence of Trp in the enzyme (IN contains six Trp residues) but not in the peptides, was exploited when performing intrinsic fluorescence quenching titrations of the former. The wt IBD is the fragment 347–471 of LEDGF (GST removed) [33,51,52]. The mutant IBD is the Asp366Asn version of the former. Like the whole protein, these contain no Trp. The concentrations of wt IN (33.781 kDa) and of the IBD fragments (16.542 kDa) were estimated from UV absorption at 280 nm, using the molar absorptivities of 46542 M^{-1} cm^{-1} and 1400 M^{-1} cm^{-1} respectively. The proteins were used in the "reaction buffer" containing 20 mM HEPES (pH 6.8), 10 mM $MgCl_2$ and 10 mM DTT.

Secondary structure predictions

Secondary structure predictions were carried out using the AGADIR and GOR IV computer programs available on the web respectively at http://www.embl-heidelberg.de/serices/serrona/agadir-start.html and http://pbil.univ-lyon1.fr/ (Pôle Bioinformatique Lyonnais, France) [63,64]. The AGADIR prediction considers short range interactions between residues and provides helical propensity per residue of peptides in solution, independently of tertiary structure interactions, with the possibility of selecting the pH and the temperature conditions. GOR IV uses parameters derived from crystallographic data of proteins. It thus provides more realistic structure predictions for peptide segments submitted to tertiary and quaternary structures constraints i.e., within the protein environment. Thus the two types of predictions can be used in conjunction to find the impact of the protein context on the secondary structure of its peptide elements, to identify the effect of mutations on secondary structures and to select the mutations that would reinforce the helicity of peptides, as was done in the case of peptide K156 (Table 1a) [43].

CD Spectroscopy

CD spectra were recorded on a Jobin-Yvon CD6 dichrograph (HORIBA Jobin-Yvon, France). Peptide concentrations varied from 5 to 25 μM in the "assay buffer", containing 40 mM sodium phosphate, 0.5 mM EDTA, pH 6.0. The samples, incubated 10 min at the chosen temperature to allow the solutions to reach their equilibrium state, were placed in thermally jacketed cells with a 1 mm path length. The spectra, recorded in 1 nm steps, were averaged over ten scans and corrected for the base line, then presented as differential molar absorptivities per residue, $\Delta\varepsilon$ (M^{-1} cm^{-1}), for peptides, and as difference spectra (complex minus DNA), for peptide-DNA complexes. For the HTHi-LTR interaction, aliquots of peptide were added to LTR34 (10 μM) and the control spectrum of unliganded LTR was subtracted from that of the complex. Recall that in a simple random coil – α helix equilibrium, the α-helix content of peptides could be approximated by the relation: $P_\alpha = -[\Delta\varepsilon_{222} \times 10]$ (P_α: percentage of α helix; $\Delta\varepsilon_{222}$: differential molar absorptivity per residue at 222 nm) [70].

Modeling

We used the Insight II® program (Accelrys Software Inc., CA, USA) to estimate distances between the various atoms in HTHi and between HTHi and the β-stands located in the proximity, using the CC IN crystal structure (PDB ID 1BIU) [20] (Fig. 1 and Table 2). Graphics was by PyMol (http://www.pymol.org) [71] with the APBS software (http://apbs.sourceforge.net/) [72].

Fluorescence Measurements

Intrinsic fluorescence quantum yield and fluorescence anisotropy studies were carried out with a Jobin-Yvon Fluoromax II instrument (HORIBA Jobin-Yvon, France) equipped with an ozone-free 150 W xenon lamp. The samples (800 μl) were placed at 5°C in thermally jacketed 1 cm×0.5 cm quartz cells. At least ten measurements for each titration point were recorded with an integration time of 5 sec.

The intrinsic fluorescence [73] of wt IN was measured at 100 nM monomer concentration, in the "reaction buffer" (see above). The Trp residues were excited at 295 nm and emission was recorded between 305 and 450 nm, with 2 nm and 5 nm excitation and emission slit widths, respectively. A maximal emission was obtained at 337 nm. Quenching of the fluorescence of IN following the addition of HTHi or of peptide α_4 (devoid of Trp) was expressed as $1\text{-}F/F_0$, where F_0 is the fluorescence of the enzyme in the absence of peptide.

Fluorescence anisotropy titration [74,75]. Fluorescein-labeled oligonucleotides were used at 20 nM in the "assay buffer" (see Table 1b and above). With fluorescein as fluorophore, excitation and emission were at 488 nm and 516 nm, with 4 nm and 5 nm slits, respectively. Peptides were added to DNA as successive aliquots. For each anisotropy measurement, the parallel $(I_{\parallel})$ and the

perpendicular ($I_{\perp}$) intensities of the background solution (i.e., buffer and protein contributions) were subtracted from those of the sample.

The fluorescence anisotropy of the fluorescein-conjugated version of HTHi (50 nM) titrated by wt and mutated IBD in the "assay buffer" was used to evaluate the K_d of the LEDGF-HTHi complex.

Acknowledgments

We thank Alan Engelman and Mohd Jamal Dar (Dana-Farber Cancer Institute and Harvard Medical School, Boston, MA, USA) for the generous gift of the wt LEDGF-IBD and of the Asp366Asn LEDGF-IBD variant. We wish also to thank Christophe Piesse and Jean-Pierre Levillain for skilled assistance in peptide synthesis and Jean-François Mouscadet for the gift of the HIV-1 integrases.

Author Contributions

Conceived and designed the experiments: HP OM SF. Performed the experiments: HM HP LZ ZH. Analyzed the data: HM HP LZ RGM OM SF. Contributed reagents/materials/analysis tools: BR. Wrote the paper: HP OM SF. As a part of PhD thesis work: HM. As Director of thesis to HM: HP. As part of a joint PhD thesis, Paris, Beyrouth: ZH.

References

1. Roth MJ, Schwartzberg PL, Goff SP (1989) Structure of the termini of DNA intermediates in the integration of retroviral DNA: dependence on IN function and terminal DNA sequence. Cell 58: 47–54.
2. Engelman A, Mizuuchi K, Craigie R (1991) HIV-1 DNA integration: mechanism of viral DNA cleavage and DNA strand transfer. Cell 67: 1211–1221.
3. Brown PO (1997) Integration. In: Coffin JM, Hughes SH, Varmus HE, eds. Retroviruses. New-York: Cold Spring Harbor Laboratory Press. pp 161–203.
4. Craigie R (2001) HIV integrase, a brief overview from chemistry to therapeutics. J Biol Chem 276: 23213–23216.
5. Craigie R (2002) Retroviral DNA integration. In: Craig NL, Craigie R, Gellert M, Lambowitz AM, eds. Mobile DNA II. Washington, DC: ASM Press. pp 613–630.
6. Goodarzi G, Im GJ, Brackmann K, Grandgenett D (1995) Concerted integration of retrovirus-like DNA by human immunodeficiency virus type 1 integrase. J Virol 69: 6090–6097.
7. Gerton JL, Brown PO (1997) The core domain of HIV-1 integrase recognizes key features of its DNA substrates. J Biol Chem 272: 25809–25815.
8. Asante-Appiah E, Skalka AM (1999) HIV-1 integrase: structural organization, conformational changes, and catalysis. Adv Virus Res 52: 351–369.
9. Mizuuchi K (1992) Polynucleotidyl transfer reactions in transpositional DNA recombination. J Biol Chem 267: 21273–21276.
10. Mizuuchi K (1992) Transpositional recombination: mechanistic insights from studies of mu and other elements. Annu Rev Biochem 61: 1011–1051.
11. Mizuuchi K (1997) Polynucleotidyl transfer reactions in site-specific DNA recombination. Genes Cells 2: 1–12.
12. Melek M, Jones JM, O'Dea MH, Pais G, Burke TR Jr, et al. (2002) Effect of HIV integrase inhibitors on the RAG1/2 recombinase. Proc Natl Acad Sci U S A 99: 134–137.
13. Debyser Z, Cherepanov P, Van Maele B, De Clercq E, Witvrouw M (2002) In search of authentic inhibitors of HIV-1 integration. Antivir Chem Chemother 13: 1–15.
14. Pommier Y, Johnson AA, Marchand C (2005) Integrase inhibitors to treat HIV/AIDS. Nat Rev Drug Discov 4: 236–248.
15. van Gent DC, Groeneger AA, Plasterk RH (1992) Mutational analysis of the integrase protein of human immunodeficiency virus type 2. Proc Natl Acad Sci U S A 89: 9598–9602.
16. van Gent DC, Oude Groeneger AA, Plasterk RH (1993) Identification of amino acids in HIV-2 integrase involved in site-specific hydrolysis and alcoholysis of viral DNA termini. Nucleic Acids Res 21: 3373–3377.
17. Esposito D, Craigie R (1999) HIV integrase structure and function. Adv Virus Res 52: 319–333.
18. Dyda F, Hickman AB, Jenkins TM, Engelman A, Craigie R, et al. (1994) Crystal structure of the catalytic domain of HIV-1 integrase: similarity to other polynucleotidyl transferases. Science 266: 1981–1986.
19. Bujacz G, Jaskolski M, Alexandratos J, Wlodawer A, Merkel G, et al. (1996) The catalytic domain of avian sarcoma virus integrase: conformation of the active-site residues in the presence of divalent cations. Structure 4: 89–96.
20. Goldgur Y, Dyda F, Hickman AB, Jenkins TM, Craigie R, et al. (1998) Three new structures of the core domain of HIV-1 integrase: an active site that binds magnesium. Proc Natl Acad Sci U S A 95: 9150–9154.
21. Greenwald J, Le V, Butler SL, Bushman FD, Choe S (1999) The mobility of an HIV-1 integrase active site loop is correlated with catalytic activity. Biochemistry 38: 8892–8898.
22. Maignan S, Guilloteau JP, Zhou-Liu Q, Clement-Mella C, Mikol V (1998) Crystal structures of the catalytic domain of HIV-1 integrase free and complexed with its metal cofactor: high level of similarity of the active site with other viral integrases. J Mol Biol 282: 359–368.
23. Chen JC, Krucinski J, Miercke LJ, Finer-Moore JS, Tang AH, et al. (2000) Crystal structure of the HIV-1 integrase catalytic core and C-terminal domains: a model for viral DNA binding. Proc Natl Acad Sci U S A 97: 8233–8238.
24. Chen Z, Yan Y, Munshi S, Li Y, Zugay-Murphy J, et al. (2000) X-ray structure of simian immunodeficiency virus integrase containing the core and C-terminal domain (residues 50–293)–an initial glance of the viral DNA binding platform. J Mol Biol 296: 521–533.
25. Wang JY, Ling H, Yang W, Craigie R (2001) Structure of a two-domain fragment of HIV-1 integrase: implications for domain organization in the intact protein. EMBO J 20: 7333–7343.
26. Cai M, Zheng R, Caffrey M, Craigie R, Clore GM, et al. (1997) Solution structure of the N-terminal zinc binding domain of HIV-1 integrase. Nat Struct Biol 4: 567–577.
27. Lodi PJ, Ernst JA, Kuszewski J, Hickman AB, Engelman A, et al. (1995) Solution structure of the DNA binding domain of HIV-1 integrase. Biochemistry 34: 9826–9833.
28. Eijkelenboom AP, Lutzke RA, Boelens R, Plasterk RH, Kaptein R, et al. (1995) The DNA-binding domain of HIV-1 integrase has an SH3-like fold. Nat Struct Biol 2: 807–810.
29. Eijkelenboom AP, van den Ent FM, Vos A, Doreleijers JF, Hard K, et al. (1997) The solution structure of the amino-terminal HHCC domain of HIV-2 integrase: a three-helix bundle stabilized by zinc. Curr Biol 7: 739–746.
30. Maroun RG, Gayet S, Benleulmi MS, Porumb H, Zargarian L, et al. (2001) Peptide inhibitors of HIV-1 integrase dissociate the enzyme oligomers. Biochemistry 40: 13840–13848.
31. Baranova S, Tuzikov FV, Zakharova OD, Tuzikova NA, Calmels C, et al. (2007) Small-angle X-ray characterization of the nucleoprotein complexes resulting from DNA-induced oligomerization of HIV-1 integrase. Nucleic Acids Res 35: 975–987.
32. Li M, Mizuuchi M, Burke TR Jr, Craigie R (2006) Retroviral DNA integration: reaction pathway and critical intermediates. EMBO J 25: 1295–1304.
33. Cherepanov P, Maertens G, Proost P, Devreese B, Van Beeumen J, et al. (2003) HIV-1 integrase forms stable tetramers and associates with LEDGF/p75 protein in human cells. J Biol Chem 278: 372–381.
34. Gao K, Butler SL, Bushman F (2001) Human immunodeficiency virus type 1 integrase: arrangement of protein domains in active cDNA complexes. EMBO J 20: 3565–3576.
35. Faure A, Calmels C, Desjobert C, Castroviejo M, Caumont-Sarcos A, et al. (2005) HIV-1 integrase crosslinked oligomers are active in vitro. Nucleic Acids Res 33: 977–986.
36. Li M, Craigie R (2005) Processing of viral DNA ends channels the HIV-1 integration reaction to concerted integration. J Biol Chem 280: 29334–29339.
37. Bera S, Vora AC, Chiu R, Heyduk T, Grandgenett DP (2005) Synaptic complex formation of two retrovirus DNA attachment sites by integrase: a fluorescence energy transfer study. Biochemistry 44: 15106–15114.
38. Karki RG, Tang Y, Burke TR Jr, Nicklaus MC (2004) Model of full-length HIV-1 integrase complexed with viral DNA as template for anti-HIV drug design. J Comput Aided Mol Des 18: 739–760.
39. Wielens J, Crosby IT, Chalmers DK (2005) A three-dimensional model of the human immunodeficiency virus type 1 integration complex. J Comput Aided Mol Des 19: 301–317.
40. Podtelezhnikov AA, Gao K, Bushman FD, McCammon JA (2003) Modeling HIV-1 integrase complexes based on their hydrodynamic properties. Biopolymers 68: 110–120.
41. Chen A, Weber IT, Harrison RW, Leis J (2006) Identification of amino acids in HIV-1 and avian sarcoma virus integrase subsites required for specific recognition of the long terminal repeat Ends. J Biol Chem 281: 4173–4182.
42. Goldgur Y, Craigie R, Cohen GH, Fujiwara T, Yoshinaga T, et al. (1999) Structure of the HIV-1 integrase catalytic domain complexed with an inhibitor: a platform for antiviral drug design. Proc Natl Acad Sci U S A 96: 13040–13043.
43. Zargarian L, Benleumi MS, Renisio JG, Merad H, Maroun RG, et al. (2003) Strategy to discriminate between high and low affinity bindings of human immunodeficiency virus, type 1 integrase to viral DNA. J Biol Chem 278: 19966–19973.
44. Jenkins TM, Esposito D, Engelman A, Craigie R (1997) Critical contacts between HIV-1 integrase and viral DNA identified by structure-based analysis and photo-crosslinking. EMBO J 16: 6849–6859.
45. Heuer TS, Brown PO (1998) Photo-cross-linking studies suggest a model for the architecture of an active human immunodeficiency virus type 1 integrase-DNA complex. Biochemistry 37: 6667–6678.

46. Esposito D, Craigie R (1998) Sequence specificity of viral end DNA binding by HIV-1 integrase reveals critical regions for protein-DNA interaction. EMBO J 17: 5832–5843.
47. Lu R, Limon A, Ghory HZ, Engelman A (2005) Genetic analyses of DNA-binding mutants in the catalytic core domain of human immunodeficiency virus type 1 integrase. J Virol 79: 2493–2505.
48. Li HY, Zawahir Z, Song LD, Long YQ, Neamati N (2006) Sequence-based design and discovery of peptide inhibitors of HIV-1 integrase: insight into the binding mode of the enzyme. J Med Chem 49: 4477–4486.
49. Maroun RG, Krebs D, Roshani M, Porumb H, Auclair C, et al. (1999) Conformational aspects of HIV-1 integrase inhibition by a peptide derived from the enzyme central domain and by antibodies raised against this peptide. Eur J Biochem 260: 145–155.
50. Maroun RG, Krebs D, El Antri S, Deroussent A, Lescot E, et al. (1999) Self-association and domains of interactions of an amphipathic helix peptide inhibitor of HIV-1 integrase assessed by analytical ultracentrifugation and NMR experiments in trifluoroethanol/H_2O mixtures. J Biol Chem 274: 34174–34185.
51. Cherepanov P, Sun ZY, Rahman S, Maertens G, Wagner G, et al. (2005) Solution structure of the HIV-1 integrase-binding domain in LEDGF/p75. Nat Struct Mol Biol 12: 526–532.
52. Cherepanov P, Ambrosio AL, Rahman S, Ellenberger T, Engelman A (2005) Structural basis for the recognition between HIV-1 integrase and transcriptional coactivator p75. Proc Natl Acad Sci U S A 102: 17308–17313.
53. Llano M, Saenz DT, Meehan A, Wongthida P, Peretz M, et al. (2006) An Essential Role for LEDGF/p75 in HIV Integration. Science.
54. Emiliani S, Mousnier A, Busschots K, Maroun M, Van Maele B, et al. (2005) Integrase mutants defective for interaction with LEDGF/p75 are impaired in chromosome tethering and HIV-1 replication. J Biol Chem 280: 25517–25523.
55. Busschots K, Voet A, De Maeyer M, Rain JC, Emiliani S, et al. (2007) Identification of the LEDGF/p75 Binding Site in HIV-1 Integrase. Journal of Molecular Biology 365: 1480–1492.
56. Pandey KK, Sinha S, Grandgenett DP (2007) Transcriptional coactivator LEDGF/p75 modulates human immunodeficiency virus type 1 integrase-mediated concerted integration. J Virol 81: 3969–3979.
57. Bouyac-Bertoia M, Dvorin JD, Fouchier RA, Jenkins Y, Meyer BE, et al. (2001) HIV-1 infection requires a functional integrase NLS. Mol Cell 7: 1025–1035.
58. Armon-Omer A, Graessmann A, Loyter A (2004) A synthetic peptide bearing the HIV-1 integrase 161–173 amino acid residues mediates active nuclear import and binding to importin alpha: characterization of a functional nuclear localization signal. J Mol Biol 336: 1117–1128.
59. Limon A, Devroe E, Lu R, Ghory HZ, Silver PA, et al. (2002) Nuclear localization of human immunodeficiency virus type 1 preintegration complexes (PICs): V165A and R166A are pleiotropic integrase mutants primarily defective for integration, not PIC nuclear import. J Virol 76: 10598–10607.
60. Dvorin JD, Bell P, Maul GG, Yamashita M, Emerman M, et al. (2002) Reassessment of the roles of integrase and the central DNA flap in human immunodeficiency virus type 1 nuclear import. J Virol 76: 12087–12096.
61. Harrison SC, Aggarwal AK (1990) DNA recognition by proteins with the helix-turn-helix motif. Annu Rev Biochem 59: 933–969.
62. Keenan RJ, Freymann DM, Walter P, Stroud RM (1998) Crystal structure of the signal sequence binding subunit of the signal recognition particle. Cell 94: 181–191.
63. Garnier J, Gibrat JF, Robson B (1996) GOR method for predicting protein secondary structure from amino acid sequence. Methods Enzymol 266: 540–553.
64. Munoz V, Serrano L (1997) Development of the multiple sequence approximation within the AGADIR model of alpha-helix formation: comparison with Zimm-Bragg and Lifson-Roig formalisms. Biopolymers 41: 495–509.
65. Krebs D, Dahmani B, Monnot M, Mauffret O, Troalen F, et al. (1996) Dissection of the basic subdomain of the c-Jun oncoprotein: a structural analysis of two peptide fragments by CD, Fourier-transform infrared and NMR. Eur J Biochem 235: 699–712.
66. Porumb H, Zargarian L, Merad H, Maroun R, Mauffret O, et al. (2004) Circular dichroism and fluorescence of a tyrosine side-chain residue monitors the concentration-dependent equilibrium between U-shaped and coiled-coil conformations of a peptide derived from the catalytic core of HIV-1 integrase. Biochim Biophys Acta 1699: 77–86.
67. Hazuda DJ, Felock P, Witmer M, Wolfe A, Stillmock K, et al. (2000) Inhibitors of strand transfer that prevent integration and inhibit HIV-1 replication in cells. Science 287: 646–650.
68. Morant-Lhomel A, René B, Zargarian L, Troalen F, Mauffret O, et al. (2006) Self-association and DNA binding properties of the human topoisomerase IIA alpha2HTH module. Biochimie 88: 253–263.
69. Leh H, Brodin P, Bischerour J, Deprez E, Tauc P, et al. (2000) Determinants of Mg2+-dependent activities of recombinant human immunodeficiency virus type 1 integrase. Biochemistry 39: 9285–9294.
70. Zhong L, Johnson WC Jr (1992) Environment affects amino acid preference for secondary structure. Proc Natl Acad Sci U S A 89: 4462–4465.
71. DeLano WL (2002) The PyMOL Molecular Graphics System, version DeLano Scientific, Palo Alto, CA, USA.
72. Baker NA, Sept D, Joseph S, Holst MJ, McCammon JA (2001) Electrostatics of nanosystems: application to microtubules and the ribosome. Proc Natl Acad Sci U S A 98: 10037–10041.
73. Eftink MR (1997) Fluorescence methods for studying equilibrium macromolecule-ligand interactions. Methods Enzymol 278: 221–257.
74. Heyduk T, Lee JC (1990) Application of fluorescence energy transfer and polarization to monitor Escherichia coli cAMP receptor protein and lac promoter interaction. Proc Natl Acad Sci U S A 87: 1744–1748.
75. Hill JJ, Royer CA (1997) Fluorescence approaches to study of protein-nucleic acid complexation. Methods Enzymol 278: 390–416.